Effective properties of two-phase disordered composite media: II. Evaluation of bounds on the conductivity and bulk modulus of dispersions of impenetrable spheres

S. Torquato
Department of Mechanical and Aerospace Engineering and Department of Chemical Engineering, North Carolina State University, Raleigh, North Carolina 27695-7910

F. Lado
Department of Physics, North Carolina State University, Raleigh, North Carolina 27695-8202
(Received 16 December 1985)

We evaluate third-order bounds on the effective conductivity σ_e and effective bulk modulus K_e of a random dispersion of equal-sized impenetrable spheres in a matrix up to sphere volume fractions near the random close-packing value. The third-order bounds, which incorporate an integral ζ_2 that depends upon the three-point probability function of the two-phase medium, are shown to significantly improve upon second-order Hashin-Shtrikman bounds, which do not utilize this information, for a wide range of phase property values and volume fractions. The physical significance of the microstructural parameter ζ_2 for general microstructures is briefly discussed. The third-order bounds on σ_e and K_e are found to be sharp enough to yield good estimates of the bulk properties for a wide range of sphere volume fractions, even when the phase property values differ by as much as two orders of magnitude. Moreover, when the spheres are highly conducting or highly rigid relative to the matrix, the third-order lower bound on the respective effective property provides a useful estimate of it for a wide range of sphere volume fractions.

I. INTRODUCTION

In a previous article[1] (henceforth referred to as I) in this series of studies of the effective properties of two-phase disordered composite media, we simplified the key multidimensional cluster integral that arises in both the third-order bounds on the effective conductivity σ_e and bulk modulus K_e due to Beran[2] and to Beran and Molyneux[3] (BM), respectively, for the model of impenetrable spherical inclusions randomly and isotropically distributed throughout a matrix. In this article, we employ the simplified integrals to evaluate these bounds on σ_e and K_e and another third-order bound on σ_e derived by Milton[4,5] for the same model.

The phase volume fractions, conductivities, bulk moduli, and shear moduli are denoted, respectively, by ϕ_1 and ϕ_2, σ_1 and σ_2, K_1 and K_2, and G_1 and G_2, where phase 1 is the matrix phase and phase 2 is the included phase. In Sec. II we present the simplified forms of the Beran, Milton, and BM bounds for an isotropic suspension of impenetrable spheres. In Sec. III we evaluate ζ_2, the key integral that is involved in all of these bounds, for this model up to a sphere volume fraction $\phi_2=0.6$. The important microstructural parameter ζ_2, which depends upon a certain three-point probability function of the composite, that is calculated here, is compared to the corresponding values associated with other model geometries. This comparison enables us to shed some light on the physical significance of ζ_2. Using the results of Sec. III, the third-order bounds on σ_e and K_e are then computed in Sec. IV, for a dispersion of impenetrable spheres up to densities near the random close-packing value. Here, we also compare our conductivity results to experimental data. In Sec. V we make some concluding remarks.

II. SIMPLIFIED BOUNDS FOR DISPERSIONS OF IMPENETRABLE SPHERES

The third-order Beran[2] bounds on the effective conductivity σ_e have been shown to depend upon σ_1, σ_2, ϕ_2, and a single integral ζ_1 (defined below) which depends upon the three-point probability function $S_3(r,s,t)$,[6,7] a quantity that gives the probability of finding in phase 1 the vertices of a triangle of edge lengths r, s, and t. The third-order BM (Ref. 3) bounds on the effective bulk modulus K_e depend upon K_1, K_2, G_1, G_2, and also upon the same integral ζ_1 that appears in the Beran bounds.[7] (Third-order bounds are exact through third order in the difference in the phase property values.) The Beran bounds on σ_e and the BM bounds on K_e are, respectively,

$$\left[\langle 1/\sigma\rangle-\frac{2\phi_1\phi_2(1/\sigma_1-1/\sigma_2)^2}{2\langle 1/\tilde{\sigma}\rangle+\langle 1/\sigma\rangle_\zeta}\right]^{-1} \le\sigma_e\le\left[\langle\sigma\rangle-\frac{\phi_1\phi_2(\sigma_2-\sigma_1)^2}{\langle\tilde{\sigma}\rangle+2\langle\sigma\rangle_\zeta}\right] \quad (2.1)$$

and

$$\left[\langle 1/K\rangle-\frac{4\phi_1\phi_2(1/K_1-1/K_2)^2}{4\langle 1/\tilde{K}\rangle+3\langle 1/G\rangle_\zeta}\right]^{-1} \le K_e\le\left[\langle K\rangle-\frac{3\phi_1\phi_2(K_2-K_1)^2}{3\langle\tilde{K}\rangle+4\langle G\rangle_\zeta}\right]. \quad (2.2)$$

For any property b, we write $\langle b\rangle = b_1\phi_1 + b_2\phi_2$, $\langle \tilde{b}\rangle = b_1\phi_2 + b_2\phi_1$, and $\langle b\rangle_\zeta = b_1\zeta_1 + b_2\zeta_2$. Moreover, we put

$$\zeta_1 = 1-\zeta_2 = \frac{9}{2\phi_1\phi_2} I_1[\hat{S}_3] , \tag{2.3}$$

$$\hat{S}_3(r_{12},r_{13},r_{23}) = S_3(r_{12},r_{13},r_{23}) - \frac{S_2(r_{12})S_2(r_{13})}{\phi_1} , \tag{2.4}$$

and

$$I_1[\,] = \frac{1}{8\pi^2}\int\int d\mathbf{r}_2 d\mathbf{r}_3[\,]\frac{P_2(\hat{r}_{12}\cdot\hat{r}_{13})}{r_{12}^3 r_{13}^3} . \tag{2.5}$$

Here S_2 is the two-point probability function, $r_{ij} = |\mathbf{r}_i - \mathbf{r}_j|$, $\hat{r}_{ij} = \mathbf{r}_{ij}/|\mathbf{r}_{ij}|$ and P_2 is the Legendre polynomial of order two. The form of Eq. (2.4) ensures that $I_1[\hat{S}_3]$, and therefore ζ_1, is absolutely convergent.

The fact that ζ_1 and hence ζ_2 lie in the closed interval [0,1] implies that the third-order Beran and BM bounds always improve upon the second-order bounds on σ_e and K_e due to Hashin and Shtrikman (HS).[8,9] Since the latter are realized for a certain composite sphere assemblage, they are the best bounds on these effective properties for a statistically isotropic two-phase composite material, given only the phase property values and ϕ_2, the simplest of the microstructural parameters of the medium. The HS upper bound on σ_e for $\sigma_2 \geq \sigma_1$, for example, corresponds to a two-phase system composed of "composite" spheres consisting of a core of conductivity σ_1 and radius R_c, surrounded by a concentric shell of conductivity σ_2 and radius R_0. The ratio $R_c^3/R_0^3 = \phi_1$ and so the composite spheres fill all space, implying that there is a distribution in their size ranging to the infinitesimally small. For $\zeta_1 = 0$ or, equivalently, for $\zeta_2 = 1$, the bounds (2.1) coincide with and are equal to the HS upper bound for $\sigma_2 \geq \sigma_1$. Hence, ζ_1 is 0 and ζ_2 is 1 for the composite sphere assemblage (CSA) described above. On the other hand, the HS lower bound on σ_e for $\sigma_2 \geq \sigma_1$ corresponds to the CSA but with phase 1 interchanged with phase 2. For $\zeta_1 = 1$ or $\zeta_2 = 0$, the bounds (2.1) coincide with and are equal to the HS lower bound when $\sigma_2 \geq \sigma_1$. Therefore, for the CSA model corresponding to the HS lower bound, $\zeta_1 = 1$ and $\zeta_2 = 0$. The HS bounds on K_e also become exact for the analogous CSA geometries. Note that the HS lower bound for $\sigma_2 \geq \sigma_1$ is equivalent to the well-known Maxwell[10] (or in the dielectric context, the Clausius-Mossotti[11]) formula. The Maxwell formula therefore corresponds to a dispersion in which the average distance between polydispersed particles is of the order $R_c\phi_2^{-1/3}$.

Milton[4,5] has derived the following third-order lower bound on the effective conductivity for $\sigma_2 \geq \sigma_1$:

$$\sigma_e \geq \sigma_1\left[\frac{(\sigma_1+2\sigma_2)(\sigma_2+2\langle\sigma\rangle) - 2\phi_1\zeta_2(\sigma_2-\sigma_1)^2}{(\sigma_1+2\sigma_2)(2\sigma_1+\langle\tilde{\sigma}\rangle) - 2\phi_1\zeta_2(\sigma_2-\sigma_1)^2}\right] . \tag{2.6}$$

This bound is exactly realized for a material composed of composite spheres consisting of a core of conductivity σ_1 and radius R_c, surrounded by a concentric shell of conductivity σ_2 and outer radius R_0, which is in turn surrounded by a concentric shell of conductivity σ_1 and outer radius R. The ratio R_c^3/R_0^3 is equal to the constant $\phi_1\zeta_2$ and the composite spheres fill all space, implying that there is a distribution in their sizes ranging to the infinitesimally small. Therefore, bound (2.6) is the best possible lower bound on σ_e given $\sigma_1, \sigma_2, \phi_2$, and ζ_2, and is always better than the Beran lower bound (2.1) for $0 < \zeta_2 < 1$.

In order to evaluate the bounds described above one must calculate $I_1[\hat{S}_3]$ and hence ζ_1 for the microgeometry of interest. In I we simplified the cluster integral $I_1[\hat{S}_3]$ for the case of a suspension of impenetrable spherical inclusions and found that for spheres of unit radius

$$I_1[\hat{S}_3] = \tfrac{2}{9}\phi_1\phi_2 - K , \tag{2.7}$$

where

$$K = \tfrac{2}{3}\phi_2^2\int_2^\infty dr\frac{r^2 g(r)}{(r^2-1)^3} + \frac{\phi_2^3}{16\pi^2}\sum_{l=2}^{\infty} l(l-1)\int\int d\mathbf{r}_2 d\mathbf{r}_3[g_3(r_{12},r_{13},r_{23}) - g(r_{12})g(r_{13})]\frac{P_l(\cos\theta_{213})}{r_{12}^{l+1}r_{13}^{l+1}} . \tag{2.8}$$

Here, $g(r)$ is the pair distribution function, $g_3(r_{12},r_{13},r_{23})$ is the three-particle distribution function, $\cos\theta_{213} = \hat{r}_{12}\cdot\hat{r}_{13}$, and P_l is the Legendre polynomial of order l. The integrals of K had been obtained earlier by Felderhof[12,13] using an approach which is completely different from the one outlined in I.

III. THREE-POINT PARAMETER ζ_2 FOR IMPENETRABLE SPHERES

A. Calculation of ζ_2

Here we calculate the three-point microstructural parameter ζ_2 for a suspension of impenetrable spherical inclusions. As noted in Eq. (2.8), for this we need the pair and triplet distribution functions[14] of hard spheres of diameter 2. The first of these is conveniently obtainable from the accurate fit of Verlet and Weis.[15] This parametrization, however, appears to break down as the random close-packing density is approached and so the highest density reported here corresponds to a sphere volume fraction $\phi_2 = 0.6$, for which the Verlet-Weis results still show their expected internal consistency.

As usual, the calculation of the triplet correlation function is more problematical. Lacking any more fundamental alternative, we have resorted to the familiar Kirkwood superposition approximation,

$$g_3(r_{12},r_{13},r_{23}) \approx g(r_{12})g(r_{13})g(r_{23}) , \tag{3.1}$$

to evaluate this quantity.

For numerical work, it is advantageous to replace $g(r)$ in the first integral of (2.8) with $1 + h(r)$ and evaluate

analytically the first of the two integrals that result. We have then

$$k_2 \equiv \tfrac{2}{3}\int_2^\infty dr \frac{r^2 g(r)}{(r^2-1)^3} = \tfrac{5}{54} - \tfrac{1}{24}\ln 3 + \tfrac{2}{3}\int_2^\infty dr \frac{r^2 h(r)}{(r^2-1)^3} , \tag{3.2}$$

where now the integrand with $h(r)$ vanishes rapidly for large r. This integral was evaluated using the trapezoidal rule with 1024 points, an interval $\Delta r = 0.01$ and, as noted, the Verlet-Weis fit[15] to $g(r)$.

In superposition approximation, the second integral of (2.8) becomes

$$k_3 \equiv \frac{1}{16\pi^2}\sum_{l=2}^{\infty} l(l-1)\int d\mathbf{r}_2 d\mathbf{r}_3 g(r_{12}) g(r_{13}) h(r_{23}) \frac{P_l(\cos\theta_{213})}{r_{12}^{l+1} r_{13}^{l+1}} = \sum_{l=2}^{\infty} \frac{l(l-1)}{2l+1}\int_2^\infty dr_{12} \frac{g(r_{12})}{r_{12}^{l-1}} \int_2^\infty dr_{13} \frac{g(r_{13})}{r_{13}^{l-1}} H_l(r_{12}, r_{13}) , \tag{3.3}$$

where

$$H_l(r_{12}, r_{13}) = \frac{2l+1}{2}\int_{-1}^{1} d(\cos\theta_{213}) h(r_{23}) P_l(\cos\theta_{213}) \tag{3.4}$$

and $r_{23}^2 = r_{12}^2 + r_{13}^2 - 2r_{12}r_{13}\cos\theta_{213}$. It was shown in Appendix A of I that the coefficient H_l could also be written as

$$H_l(r_{12}, r_{13}) = \frac{2l+1}{2\pi^2}\int_0^\infty dk\, k^2 \tilde{h}(k) j_l(kr_{12}) j_l(kr_{13}) , \tag{3.5}$$

where $\tilde{h}(k)$ is the Fourier transform of $h(r)$ and j_l the spherical Bessel function of order l. With this result, (3.3) becomes

$$k_3 = \frac{1}{2\pi^2}\sum_{l=2}^{\infty} l(l-1)\int_0^\infty dk\, k^2 \tilde{h}(k)[F_l(k)]^2 , \tag{3.6}$$

with

$$F_l(k) = \int_2^\infty dr\, g(r)\frac{j_l(kr)}{r^{l-1}} = \frac{j_{l-1}(2k)}{2^{l-1}k} + \int_2^\infty dr\, h(r)\frac{j_l(kr)}{r^{l-1}} . \tag{3.7}$$

Equation (3.6) is also the final form used by Felderhof.[13] The integrals in (3.6) and (3.7) were again evaluated using the trapezoidal rule with 1024 points, $\Delta r = 0.01$, and $\Delta k = \pi/(1024\Delta r)$. The summation in (3.6) was continued until new terms did not affect the fifth decimal place of the sum; this requires up to ten terms in the sum at the highest density reported.

B. Results and discussion

In Table I the three-point parameter $\zeta_2 = 1 - \zeta_1$ for the model of impenetrable spherical inclusions randomly and isotropically distributed throughout a matrix is tabulated at selected values of ϕ_2 in the range $0 \le \phi_2 \le 0.6$. It should be noted that recent findings[16,17] strongly indicate that the use of the superposition approximation in the second integral of K, Eq. (2.8), underestimates the actual value of ζ_2 for arbitrary ϕ_2, with the largest deviation occurring at the maximum value of $\phi_2 \approx 0.64$ (i.e., the random close-packing value[18]). The error introduced in using the superposition approximation to evaluate K and thus ζ_2 cannot be fully determined for all ϕ_2 until the nontrivial three-body integral is evaluated using computer simulation techniques. At any rate, the use of a lower bound on ζ_2 in third-order bounds still gives rigorous bounds on the effective properties, albeit bounds weaker than ones employing the exact ζ_2.

The physical significance of the three-point parameter ζ_2 has yet to be fully elucidated for arbitrary composite media. Some physical insight can be gained by comparing our results for random impenetrable spheres to the relatively few calculations of ζ_2 for other microstructures. For Bruggeman's[19] symmetric effective-medium approximation (EMA), $\zeta_2 = \phi_2$ for spherical grains.[20] Recently, Milton[5,21] has shown that the EMA is exact, after certain limits have been taken, for a class of granular aggregates, such that there is no correlation between the location of the two types of grains and that grains of comparable size are well separated. Milton[21] also has noted that this class of two-phase media is related to Miller's[22] symmetric-cell materials for which ζ_2 is also equal to ϕ_2 for spherical cells. These materials are constructed by tessellating space into cells of various shapes and sizes, with cells randomly and independently designated as phase 1 or phase 2 with probabilities ϕ_1 and ϕ_2, respectively. The three-point

TABLE I. Three-point parameter ζ_2 for an equilibrium distribution of equal-sized impenetrable spheres in a matrix.

ϕ_2	ζ_2
0.0	0.0
0.05	0.010 41
0.10	0.020 53
0.15	0.030 33
0.20	0.039 83
0.25	0.049 16
0.30	0.058 75
0.35	0.069 54
0.40	0.083 56
0.45	0.1051
0.50	0.1407
0.55	0.2051
0.60	0.3277

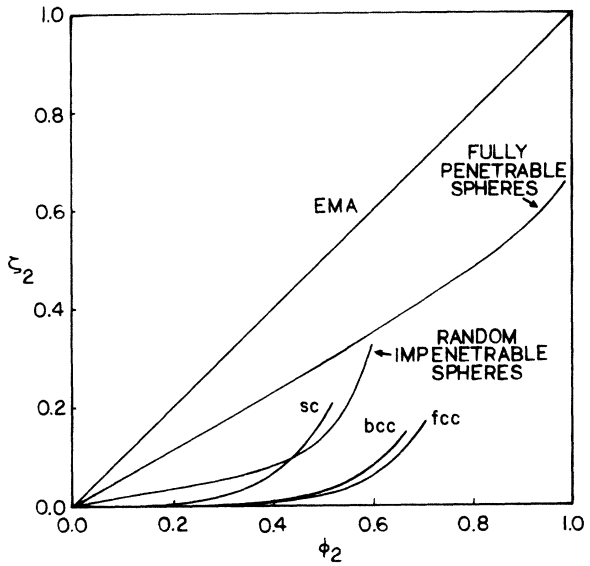

FIG. 1. Three-point parameter ζ_2 for three periodic arrays of spheres (Ref. 23) [simple cubic (sc), body-centered cubic (bcc), and face-centered cubic (fcc)], fully penetrable spheres (Refs. 6 and 24), the class of models corresponding to the EMA, and the random impenetrable-sphere model calculated here.

parameter has also been determined for periodic arrays of spheres[23] and for fully penetrable spheres[6,24] (i.e., randomly centered spheres).

In Fig. 1 the three-point parameter ζ_2 is given as a function of ϕ_2 for (i) three cubic arrays of spheres[23] (up to ϕ_2 very near the close-packing values), (ii) fully penetrable spheres,[6,24] (iii) granular materials corresponding to the EMA (which is equal to the one for symmetric-cell materials), and (iv) the equilibrium distribution of impenetrable spheres studied here. Recall that the deviation of ζ_2 from 0 and 1 is a measure of the microstructural differences between the model of interest and the Hashin-Shtrikman CSA geometries in which phase 2 and phase 1 are the dispersed phases, respectively.

Note that for all the models depicted in Fig. 1, ζ_2 is a monotonically increasing function of ϕ_2 with $\zeta_2=0$ at $\phi_2=0$. For general dispersions, $\zeta_2'(\phi_2=0)$ depends only upon the shape of the inclusion[7,25] and hence is independent of the size distribution.

Torquato[25] has shown that the slope of ζ_2 at $\phi_2=0$, $\zeta_2'(\phi_2=0)$, for dispersions depends not only upon the shape of the inclusion but upon the zero-density limit of the radial distribution function $g_0(r)$, which can be written as a sum of the zero-density limits of the pair-blocking $g_0^*(r)$ and pair-connectedness $g_0^+(r)$ functions. (The pair-blocking and pair-connectedness functions are the probability densities associated with finding two sphere centers, separated by a distance r, not belonging and belonging to the same cluster, respectively.)[26] More precisely, $\zeta_2'(\phi_2=0)$ depends upon multidimensional integrals possessing positive integrands proportional to $g_0(r)=g_0^*(r)+g_0^+(r)$. Unlike the case of random impenetrable spheres for which $g_0(r)=g_0^*(r)$, both $g_0^*(r)$ and $g_0^+(r)$ are nonzero and positive for fully penetrable spheres. It is for this reason that $\zeta_2'(\phi_2=0)$ for the former (0.210 68) is smaller than the corresponding slope for the latter (0.561 46). Similarly, since for a dilute dispersion of random impenetrable spheres ($\phi_2 \ll 1$) the second sphere relative to the first occupies all allowable positions with equal probability [i.e., $g_0(r)=g_0^*(r)$ is equal to unity if $r \geq 2a$ and zero otherwise, where a is the sphere radius] and for periodic arrays of impenetrable spheres $g_0(r)=g_0^*(r)=0$ for r less than distances of the order $a\phi_2^{-1/3}$, then $\zeta_2'(\phi_2=0)=0$ for periodic arrays since $a\phi_2^{-1/3} \gg 1$. Hence, because the impenetrable particles of periodic systems are well separated at low sphere concentrations, the expansion of ζ_2 through first order in ϕ_2 for these models is equal to that of the CSA model in which phase 2 is the dispersed phase. Although the microstructures of the family of models corresponding to the EMA and the fully penetrable-sphere model are characterized by a high degree of "randomness," the former, unlike the latter, is composed of grains with a distribution of sizes such that grains of comparable size are well separated. This difference will clearly be reflected in $g_0^*(r)$ and $g_0^+(r)$ for these two cases and presumably is the reason why $\zeta_2'(\phi_2=0)$ for the EMA is larger than $\zeta_2'(\phi_2=0)$ for fully penetrable spheres. These two-body correlation functions for EMA geometries have yet to be determined, however.

It is interesting to note that ζ_2 for the EMA is exactly linear in ϕ_2 and hence is completely determined by the zero-density limits of the pair-blocking and pair-connectedness functions. Moreover, ζ_2 for fully penetrable spheres is nearly linear over the entire range of ϕ_2. It is noteworthy and perhaps significant that the percolation threshold occurs at $\phi_2=\frac{1}{3}$ for the EMA models (in which phase 2 is the perfectly conducting phase) and at $\phi_2 \simeq 0.3$ for fully penetrable spheres.[27] In contrast, for the models involving equal-sized impenetrable spheres (i.e., random and periodic systems), the percolation thresholds occur at the respective close-packing sphere volume fractions where ζ_2 is a maximum. Unlike regular arrays of spheres, ζ_2 for random impenetrable spheres is approximately linear for $0 \leq \phi_2 < 0.4$. It is apparently exclusion-volume effects present in the random and periodic arrangements of impenetrable spheres that causes ζ_2 to sharply rise as ϕ_2 approaches its close-packing value.

IV. EVALUATION OF BOUNDS ON THE CONDUCTIVITY AND BULK MODULUS OF A DISPERSION OF IMPENETRABLE SPHERES

Third-order bounds on σ_e and on K_e are evaluated for a distribution of equal-sized random impenetrable spheres in a matrix for $0 \leq \phi_2 \leq 0.6$ using the results summarized in Table I. It is useful to first comment on the general utility of bounds when the phase property values widely differ. For the case of conduction, all nth-order lower bounds (where n is finite) tend to zero as $\alpha \to 0$ and all nth-order upper bounds tend to infinity as $\alpha \to \infty$, where $\alpha=\sigma_2/\sigma_1$. Similarly, for the elasticity problem, all nth-order lower bounds tend to zero as $G_2/G_1 \to 0$ (i.e., when phase 2 is a void phase) and all nth-order upper bounds tend to infinity as $G_2/G_1 \to \infty$ (i.e., when phase 2 is infinitely more rigid than phase 1). This does not mean that

bounds cannot be employed to estimate σ_e, however. For example, Torquato[16] has recently observed that lower-order lower bounds (such as second-, third-, and fourth-order bounds) should yield good estimates of σ_e/σ_1 for $\alpha \gg 1$, provided that ϕ_2 is below its percolation-threshold value and the mean cluster size[26] of phase 2, Λ_2, is much smaller than the scaled characteristic length of the composite sample L.[28] For periodic arrays of spheres and for an equilibrium distribution of impenetrable spheres, the condition that $\Lambda_2 \ll L$ is satisfied for all ϕ_2, except at the close-packing or percolation-threshold value for such systems. Similarly, lower-order upper bounds should provide useful estimates of σ_e/σ_1 for $\alpha \gg 1$, provided that ϕ_2 is above its percolation-threshold value and $\Lambda_1 \ll L$, where Λ_1 is the mean cluster size of phase 1. The accuracy of the lower-order bounds of course will improve as n increases. Analogous statements apply as well to bounds on K_e.

For example, even though lower-order upper bounds on K_e become very large when phase 2 is highly rigid relative to phase 1 ($G_2 \gg G_1$), lower-order lower bounds on K_e should yield good estimates of K_e for this case, provided that ϕ_2 is below its percolation-threshold value and that $\Lambda_2 \ll L$. Similar statements can be made regarding the utility of lower-order bounds for dispersions in which $\sigma_2 \ll \sigma_1$ and $G_2 \ll G_1$.

We first consider evaluating the third-order bounds on the effective conductivity of suspensions of impenetrable spheres. The most interesting cases for the conduction problem occur when the spheres are more conducting than the matrix ($\alpha > 1$). (For the opposite case of nonconducting impenetrable spheres in a matrix, the effective conductivity is insensitive to the details of the microstructure and hence the simple Maxwell result or, equivalently, the HS upper bound provides an excellent estimate of σ in such cases.[29]) For most values of α and ϕ_2, the Milton lower bound (2.6) is only marginally better than the Beran lower bound (2.1). When both α and ϕ_2 are large, however, the Milton lower bound is appreciably sharper. For example, when $\alpha = \infty$ and $\phi_2 = 0.6$ for the random distribution of impenetrable spheres studied here, (2.1) and (2.6) yield the lower bound on σ_e/σ_1 equal to 6.96 and 7.69, respectively.

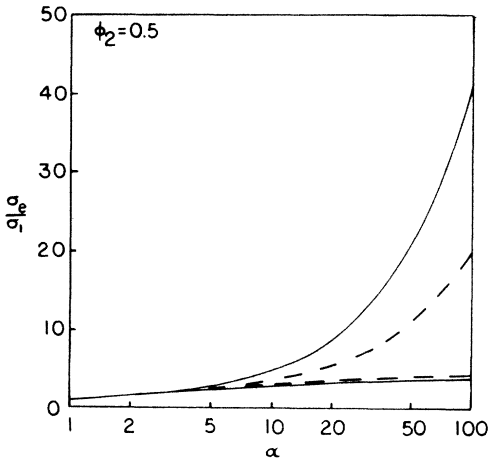

FIG. 3. As for Fig. 2 with $\phi_2 = 0.5$.

Figures 2 and 3 compare the second-order HS bounds on σ_e/σ_1 to the Beran upper bound (2.1) and the Milton lower bound (2.6) for an equilibrium distribution of impenetrable spheres in a matrix for $1 \leq \alpha \leq 100$ at $\phi_2 = 0.2$ and $\phi_2 = 0.5$, respectively. For finite α, it is seen that the third-order bounds, which include information about the three-point probability function S_3 for the model as embodied in ζ_2, always improve upon the second-order HS bounds, which do not incorporate this information. Most of this improvement is due primarily to a dramatic improvement of the upper bound, rather than the lower bound. For low to moderate sphere concentrations, the third-order lower bounds are sharp enough to provide

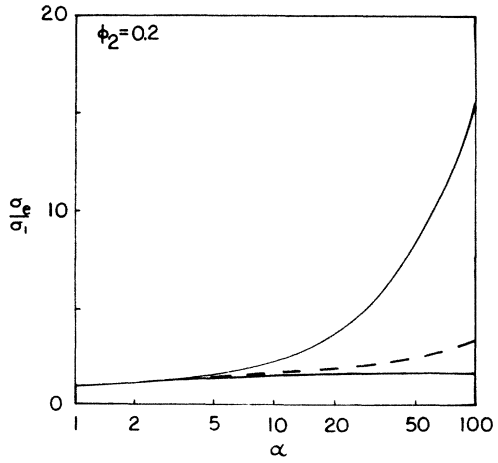

FIG. 2. Upper and lower bounds on the reduced effective conductivity σ_e/σ_1 for the range $1 \leq \alpha \leq 100$ at $\phi_2 = 0.2$. —— HS (Ref. 8) bounds; — — — Beran (Ref. 2) upper bound (2.1) and Milton (Refs. 4 and 5) lower bound (2.6) for the random impenetrable-sphere model. Here, $\alpha = \sigma_2/\sigma_1$.

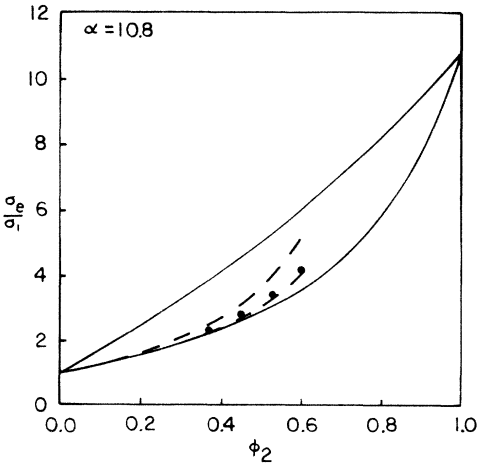

FIG. 4. Upper and lower bounds on the reduced effective conductivity σ_e/σ_1 as a function of the sphere volume fraction ϕ_2 at $\alpha = 10.8$. —— HS bounds; — — — Beran upper bound (2.1) and Milton lower bound (2.6) for the random impenetrable-sphere model. Solid circles are Turner's data (Ref. 29) for a fluidized bed of equal-sized impenetrable spheres.

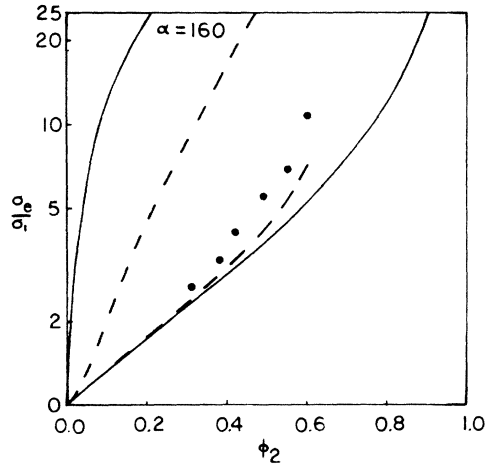

FIG. 5. As for Fig. 4 with $\alpha=160$.

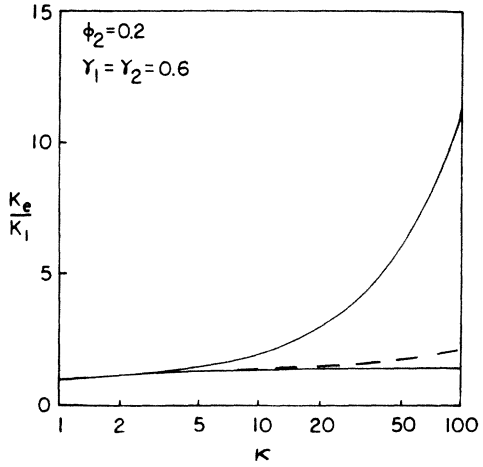

FIG. 7. Upper and lower bounds on the reduced effective bulk modulus K_e/K_1 for the range $1\leq\kappa\leq100$ at $\phi_2=0.2$. —— HS (Ref. 9) bounds; — — — BM (Ref. 3) bounds for the random impenetrable-sphere model. Here, $\kappa=K_2/K_1$, $\gamma_1=G_1/K_1=0.6$, and $\gamma_2=G_2/K_2=0.6$, and hence $\beta=G_2/G_1=\kappa$. On the scale of this figure, the third-order lower bound is indistinguishable from the second-order lower bound.

good estimates of σ_e/σ_1 when the particles are two orders of magnitude more conducting than the matrix phase. When the sphere volume fraction is large, the third-order bounds are not as restrictive; nonetheless, they provide useful estimates of the effective conductivity for the range $1\leq\alpha\leq100$.

Figures 4–6 show the Beran upper bound (2.1) and the Milton lower bound (2.6) on σ_e/σ_1 for our equilibrium impenetrable-sphere model for $\alpha=10.8$, 160, and ∞, respectively. Included in these figures are the HS second-order bounds and Turner's measurements of the reduced electrical conductivity σ_e/σ_1 of a fluidized bed of equal-sized impenetrable spheres.[29] It is not fully clear whether the static and random distribution of impenetrable spheres implied by an equilibrium distribution of such spheres is a good model of a fluidized bed of impenetrable spheres for all ϕ_2. However, we are not aware of any better data available for comparison to the model examined here for the wide parameter range of interest.

The third-order lower bound rather than the third-order upper bound provides the best agreement with Turner's experimental data for the three cases depicted in the figures, as expected. For $\alpha=10.8$, Fig. 2 shows that Milton's lower bound is in excellent agreement with the measured conductivity values. Although the correspondence between the third-order lower bound for our model and the fluidized-bed data is not as close for the cases $\alpha=160$ (Fig. 3) and $\alpha=\infty$ (Fig. 4), the lower bound does yield a reasonable estimate of the measured values, the greatest discrepancy occurring at very high sphere concentrations. The largest deviation is expected to occur when both α and ϕ_2 are very large since the effective conductivity is most sensitive to the details of the microstructure for this parameter range. However, the discrepancy between the third-order lower bound and the data in such cases can also be due to two other important factors that

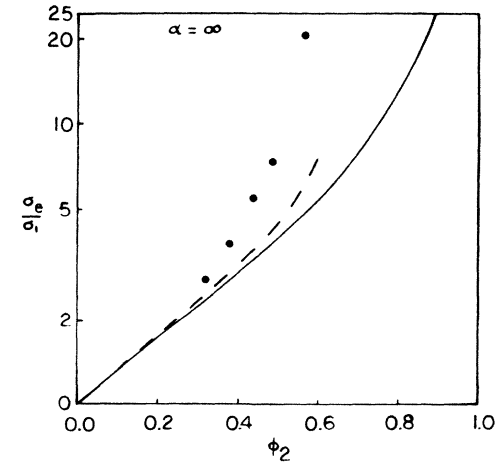

FIG. 6. As for Fig. 4 with $\alpha=\infty$. Turner's data is for $\alpha=14400$. The second- and third-order upper bounds do not appear here since they become infinite in the limit $\alpha\rightarrow\infty$.

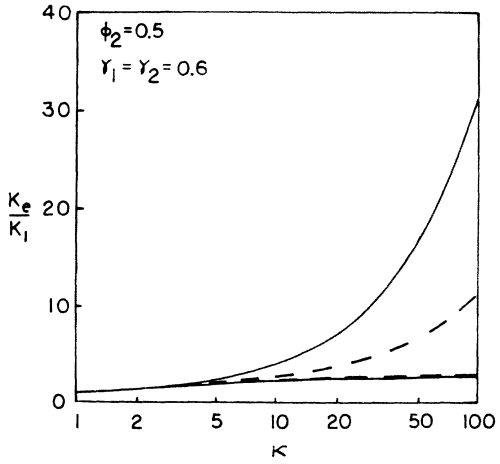

FIG. 8. As for Fig. 7 with $\phi_2=0.5$.

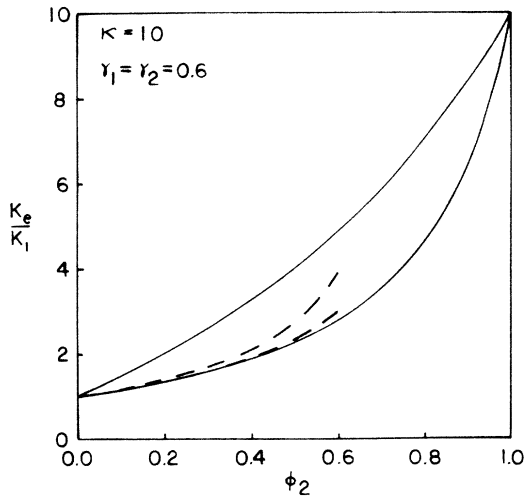

FIG. 9. Upper and lower bounds on the reduced effective bulk modulus K_e/K_1 as a function of the sphere volume fraction at $\kappa=K_2/K_1=10$ and $\beta=G_2/G_1=10$. —— HS bound; — — — BM bounds for the random impenetrable-sphere model. Here, $\gamma_1=\gamma_2=0.6$.

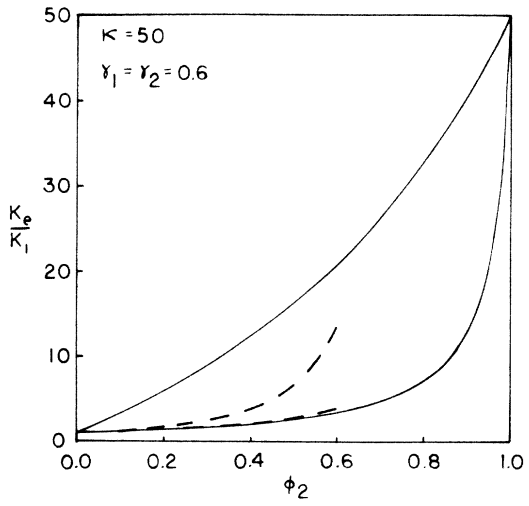

FIG. 10. As for Fig. 9 with $\kappa=\beta=50$.

we have already discussed. First, it is not wholly clear to what extent a fluidized bed is well represented by an equilibrium model. Second, the use of the superposition approximation to compute ζ_2 is expected to underestimate ζ_2 (Ref. 16) and hence underestimate the third-order lower bound.

Fourth-order lower bounds on σ_e of course should provide an even better estimate on the effective conductivity. Indeed, a highly accurate expression for the conductivity of dispersions in which $\Lambda_2 \ll L$ has recently been derived employing a rigorous fourth-order lower bound on σ_e[16].

We now turn our attention to the evaluation of the BM bounds on the effective bulk modulus for suspensions of random impenetrable spheres. It is useful to define the following parameters: $\kappa=K_2/K_1$, $\beta=G_2/G_1$, $\gamma_1=G_1/K_1$, and $\gamma_2=G_2/K_2$. Only three of these ratios are independent since $\kappa\gamma_1=\beta\gamma_2$. Moreover, because $\gamma=(3-6\nu)/(2\nu+2)$, where ν is Poisson's ratio and $0\le\nu\le 0.5$, then $0\le\gamma\le 1.5$.

In Figs. 7 and 8 we compare the second-order HS (Ref. 9) bounds on K_e/K_1 to the third-order BM bounds for an equilibrium distribution of impenetrable spheres in a matrix for $1\le\kappa=\beta\le 100$ at $\phi_2=0.2$ and 0.5, respectively. These bounds are also given as a function of the sphere volume fraction for $\kappa=\beta=10$ and $\kappa=\beta=50$ in Figs. 9 and 10, respectively. In all of these four cases $\gamma_1=\gamma_2=0.6$. The behavior of the third-order BM bounds for random suspensions of impenetrable spheres relative to the second-order HS bounds on K_e/K_1 is qualitatively similar to the behavior of the third-order bounds on σ_e for this model relative to the corresponding second-order HS (Ref. 8) bounds.

Results corresponding to Figs. 7–10 for the cases in which the particle phase is less stiff than the matrix phase are not presented here. It should be noted that in these instances, however, most of the improvement derived in using the third-order bounds is due generally to a significant improvement of the lower bound, rather than the upper bound.

V. CONCLUSIONS

In general, it is desirable to relate the effective property of a composite material to its microstructure; one then can relate changes in the microstructure quantitatively to changes in the bulk properties of the medium. Apart from a few special cases, however, the infinite set of statistical functions that characterize the microstructure (i.e., the n-point probability functions $S_1, S_2, \ldots, S_n$, $n\to\infty$) is never known. Rigorous bounds provide a means of estimating the effective property using limited microstructural information on the composite. The bounds examined here require not only the volume fraction ϕ_2 but an integral ζ_2 which depends upon S_3. For the model of an equilibrium distribution of impenetrable spheres, the third-order bounds on σ_e and K_e are found to be restrictive enough to yield good estimates of the bulk properties for the entire range of ϕ_2, even when the phase property values differ by as much as two orders of magnitude. Moreover, when the spheres are highly conducting or rigid relative to the matrix, the third-order lower bound on the respective effective property provides a reasonable estimate of it for a wide range of ϕ_2.

We are currently in the process of obtaining analogous results for the effective shear modulus. Moreover, we shall also compute third-order bounds on the conductivity and elastic moduli of the two-dimensional analogue of the model studied here (i.e., random distribution of impenetrable disks).

ACKNOWLEDGMENTS

S. T. gratefully acknowledges support of the Office of Basic Energy Sciences, U.S. Department of Energy, under Grant No. DEFG05-86ER13482. F. L. wishes to acknowledge the support of the National Science Foundation under Grant No. CHE-84-02144.

[1]F. Lado and S. Torquato, Phys. Rev. B **33**, 3370 (1986).
[2]M. Beran, Nuovo Cimento **38**, 771 (1965).
[3]M. Beran and J. Molyneux, Q. Appl. Math. **24**, 107 (1965).
[4]G. W. Milton, J. Appl. Phys. **52**, 5294 (1981).
[5]G. W. Milton, in *Physics and Chemistry in Porous Media, (Schlumberger-Doll Research)*, edited by D. L. Johnson and P. N. Sen (A.I.P., New York, 1984).
[6]S. Torquato and G. Stell (unpublished); S. Torquato and G. Stell, Lett. Appl. Eng. Sci. **23**, 375 (1985).
[7]G. W. Milton, Phys. Rev. Lett. **46**, 542 (1981).
[8]Z. Hashin and S. Shtrikman, J. Appl. Phys. **33**, 3125 (1962).
[9]Z. Hashin and S. Shtrikman, J. Mech. Phys. Solids **11**, 127 (1963).
[10]J. C. Maxwell, *Electricity and Magnetism* (Clarendon, London, 1873).
[11]R. Landauer, *Electrical Transport and Optical Properties of Inhomogeneous Media*, edited by J. C. Garland and D. B. Tanner (A.I.P., New York, 1978).
[12]B. U. Felderhof, J. Phys. C **15**, 3943 (1982).
[13]B. U. Felderhof, J. Phys. C **15**, 3953 (1982).
[14]J. P. Hansen and I. R. McDonald, *Theory of Simple Liquids* (Academic, New York, 1976).
[15]L. Verlet and J. J. Weis, Phys. Rev. A **5**, 939 (1972).
[16]S. Torquato, J. Appl. Phys. **58**, 3790 (1985).
[17]J. D. Beasley and S. Torquato (unpublished).
[18]J. G. Berryman, Phys. Rev. A **27**, 1053 (1983).
[19]D. A. G. Bruggerman, Ann. Phys. (Leipzig) **24**, 636 (1935).
[20]W. F. Brown, J. Chem. Phys. **23**, 1514 (1955).
[21]G. W. Milton, Ph.D. thesis, Cornell University, 1984.
[22]M. Miller, J. Math. Phys. **10**, 1988 (1969).
[23]R. C. McPhedran and G. W. Milton, Appl. Phys. A **26**, 207 (1981).
[24]S. Torquato and G. Stell, J. Chem. Phys. **79**, 1505 (1983).
[25]S. Torquato, J. Chem. Phys. **83**, 4776 (1985).
[26]A. Coniglio, U. DeAngelis, and A. Forlani, J. Phys. A **10**, 1123 (1977).
[27]See, for example, S. W. Haan and R. Zwanzig, J. Phys. A **10**, 1547 (1977), and references therein.
[28]The scaled characteristic length of the composite sample L is defined to be the dimensional characteristic length of the sample divided by the microscopic length scale associated with inhomogeneities. For example, for dispersions of inclusions the microscopic length scale is equal to the characteristic length of an inclusion.
[29]J. C. R. Turner, Chem. Eng. Sci. **31**, 487 (1976).